II. GROSS-PITAEVSKII EQUATION

In the mean field approximation, the packet wave functions are governed by the Gross-Pitaevskii equation [16]

$$i\hbar\frac{d\psi}{dt} = \left[-\frac{\hbar^2}{2m}\nabla^2 + V_{\rm trap}(\mathbf{r}) + \frac{4\pi\hbar^2 a}{m}|\psi|^2\right]\psi. \qquad (4)$$

Here $V_{\rm trap}(\mathbf{r})$ represents the three dimensional trapping potential in which the packets move. In accord with most experimental efforts, we assume it to be harmonic,

$$V_{\rm trap}(\mathbf{r}) = \frac{m}{2}\left(\omega_x^2 x^2 + \omega_y^2 y^2 + \omega_z z^2\right). \qquad (5)$$

The mean trap frequency is then $\omega \equiv (\omega_x\omega_y\omega_z)^{1/3}$. We consider ^{87}Rb atoms with scattering length $a = 5.77$ nm.

In an interferometer experiment, the initial condensate is the equilibrium solution to (4) with N atoms, $\psi_0(\mathbf{r})$. The optical pulse splits this into two packets ψ_+ and ψ_- moving at velocities $\pm 2\hbar k/m$ along z. As the packets move apart, they initially interact with each other. However, in a long-duration interferometer the time that the packets interact is only a small fraction of the total. We therefore neglect this interaction effect, as did IZ. Instead we solve (4) for a single packet $\psi_+(\mathbf{r}, t)$ with an atom number N_+ typically near $N/2$, and an initial state $\psi_+(\mathbf{r}, 0) = \psi_0(\mathbf{r})$. By using a Galilean transformation to the frame of the moving packet, we can treat ψ_+ as being at rest. However, since the equilibrium wave function depends on the atom number, the time evolution of ψ_+ remains nontrivial.

To perform the calculation, we first determine ψ_0 using an imaginary-time propagation technique [17]. We use the Thomas-Fermi wave function as an initial guess and propagate until the energy converges. The atom number is then suddenly reduced to N_+ and the equation is propagated forward in real time.

For propagation, we use the Strang-splitting technique outlined in [18], which is a mixed Fourier and real-space approach. We use a three-dimensional grid of 128^3 points, restricted to one octant by symmetry. Depending on the parameters, a simulation takes about an hour to run on a desktop computer.

Figure 1 shows a typical result for the rms packet width as a function of time. Since the packet is initially out of equilibrium, we observe large amplitude oscillations in all three dimensions. The dominant observed frequencies are the quadrupole modes [16], but these oscillations are anharmonic, leading to the complex structure shown.

III. PHASE DIFFUSION

The phase diffusion effect does not appear in the Gross-Pitaevskii equation (4), since phase diffusion requires a superposition of different atom numbers. However, the solution for the packet wave function ψ_+ makes evaluation of the IZ visibility, Eq. (1), straightforward. In fact,

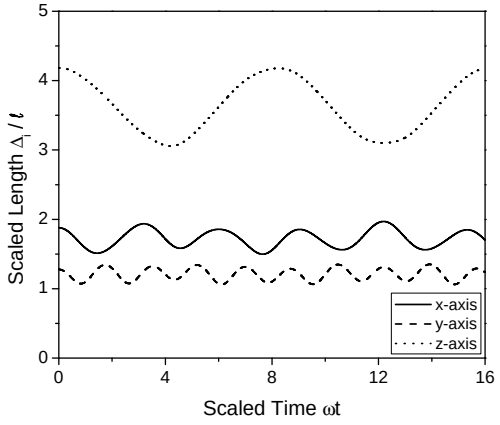

FIG. 1: Packet dynamics in a condensate interferometer. The graph shows the results obtained by numerical solution of the Gross-Pitaevskii equation for a ^{87}Rb condensate with initial atom number $N = 10^4$ in a harmonic trap with frequencies $(\omega_x, \omega_y, \omega_z) = 2\pi \times (3, 5, 1.2)$ Hz. Here the Δ_i are the root-mean-square packet widths along direction i, scaled by the harmonic oscillator length $\ell = \sqrt{\hbar/m\omega}$. At time $t = 0$ the number of atoms is suddenly reduced by a factor of two.

the IZ calculation assumes that the wave functions $\psi_\pm$ do not depend on the precise value of $N_\pm$, and that the number sensitivity enters only through the phase evolution. This assumption is essential for obtaining the simple result (1). On the one hand, it is reasonable since the fluctuations in atom number, of order $\sqrt{N}$, are very small compared to N_+ when $N \gg 1$. On the other hand, the Gross-Pitaevskii equation does depend on the atom number, so after a sufficiently long time the wave functions ψ_+ and ψ_- should begin to diverge if $N_+ \neq N_-$. These views are consistent if the time required for the wave functions to diverge is long compared to the phase diffusion time.

We were able to verify this assumption, by calculating the overlap $|\langle\psi_+|\psi_-\rangle|^2$ between a packet with $N_+ = N/2 + \sqrt{N}$ and another with $N_- = N/2 - \sqrt{N}$. The results are shown in Fig. 2 for two sets of parameters. The first corresponds to the experiments of [4]. Here the overlap remains close to one at all plausible times. The second parameters correspond to the experiments of [5]. Here the overlap does decrease, though only by about 15% at most. The time scale for the decrease is several seconds, which is about an order of magnitude longer than the diffusion time calculated below. The revival of the overlap at $T = 17$ s is due to a rephasing of the packet oscillation modes.

These two sets of parameters represent the weakest and strongest interaction strengths so far realized in this type of experiment. We therefore confirm that under typical conditions, the assumption used by IZ is valid.

IZ proposed a Thomas-Fermi approximation for ξ in

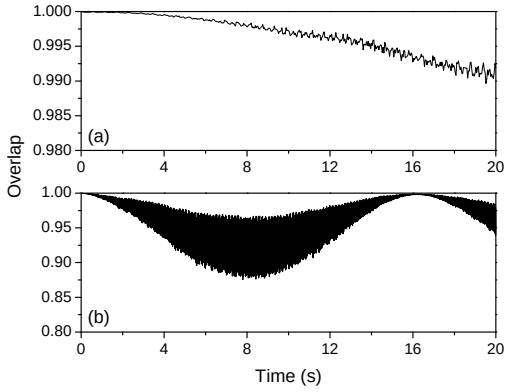

FIG. 2: Dependence of wave packet evolution on condensate number. The plots show the overlap $|\langle\psi_+|\psi_-\rangle|^2$ between two wave packets evolving as in Fig. 1, but where $\psi_\pm$ has an atom number of $N/2 \pm \sqrt{N}$. Graph (a) uses $N = 10^4$ ^{87}Rb atoms and $(\omega_x, \omega_y, \omega_z) = 2\pi \times (3, 5, 0.2)$ Hz, corresponding to the experiments of [19]. Graph (b) uses $N = 3 \times 10^3$ ^{87}Rb atoms and $(\omega_x, \omega_y, \omega_z) = 2\pi \times (60, 60, 17)$ Hz, corresponding the experiments of [5]. The curve in (b) appears thick due to rapid oscillations at the trap frequency time scale.

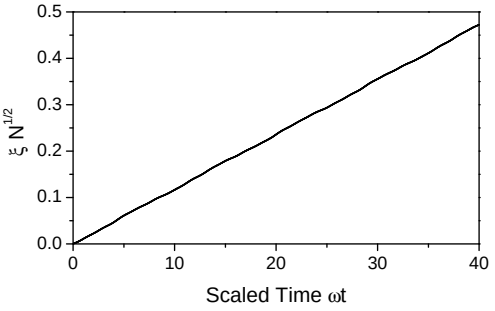

FIG. 3: Time evolution of the interaction phase. The phase parameter ξ of (3) is calculated for $N = 10^4$ ^{87}Rb atoms in a trap with $(\omega_x, \omega_y, \omega_z) = 2\pi \times (3, 5, 1.2)$ Hz. The dominant behavior is the linear increase in time. The oscillations around this behavior are small enough to neglect without significant loss of accuracy.

(2), by taking $\psi_+(\mathbf{r}, t)$ to be the stationary Thomas-Fermi wave function for $N_+ = N/2$ atoms. This leads to

$$\xi \approx 0.64 \left(\frac{a}{\ell}\right)^{2/5} \omega T N^{-3/5} \tag{6}$$

where $\ell \equiv (\hbar/m\omega)^{1/2}$ and the numerical factor is $(1800/16807)^{1/5}$. It is also possible to evaluate ξ in the limit of small interactions, where ψ_+ can be approximated by the non-interacting harmonic oscillator wave function. Here we obtain

$$\xi \approx \frac{1}{\sqrt{2\pi}} \frac{a}{\ell} \omega T. \tag{7}$$

In both of these cases, ξ depends linearly on T, leading to a visibility that decays as

$$V = \exp\left(-\frac{2T^2}{\tau^2}\right) \tag{8}$$

for a diffusion time τ. The Thomas-Fermi approximation gives

$$\tau_{\rm TF} = 1.56 \left(\frac{\ell}{a}\right)^{2/5} \frac{N^{1/10}}{\omega}. \tag{9}$$

while the weak interaction limit gives

$$\tau_0 = \sqrt{2\pi} \frac{\ell}{a\omega N^{1/2}}. \tag{10}$$

In general, however, ξ has a more complicated time dependence since g can exhibit oscillations as the packet evolves. These oscillations are in fact fairly modest under all the conditions we considered, as illustrated in Fig. 3. We therefore approximate ξ with a linear fit and obtain a diffusion time

$$\tau = N^{-1/2} \left\langle \frac{d\xi}{dt} \right\rangle^{-1}. \tag{11}$$

The brackets here represent a time average as determined by the slope of the fit line.

IV. DIFFUSION TIME RESULTS

We investigated how the diffusion time depends on the various parameters. Figure 4 illustrates the dependence on atom number N, trap frequency ω, and trap asymmetry $\lambda = \omega_x/\omega_z$ for a cylindrical trap with $\omega_y = \omega_x$. The general trends agree with expectations: The diffusion time scales rapidly with ω since a tighter trap leads to higher atom density. For large atom numbers, τ increases slowly with N owing to the interplay between the increasing density in the Thomas-Fermi wave function and the decreasing relative impact of the $\sqrt{N}$ number fluctuations. The diffusion time also increases at low atom numbers as the interaction are reduced. The diffusion time depends only weakly on the trap symmetry, in accord with the Thomas-Fermi result and weak-interaction results.

As seen, the results agree well with the Thomas-Fermi approximation at larger N, where the approximation is expected to hold. At low N, the results converge to the weak-interaction result. The crossover between these regimes is governed by the healing length $\zeta = (8\pi na)^{-1/2}$, for the atomic density n. The Thomas-Fermi approximation is good when ζ is small compared to the wavepacket size, and interactions are weak when ζ

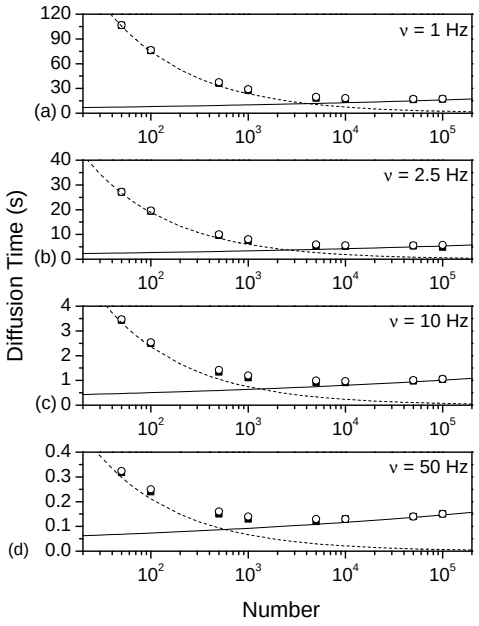

FIG. 4: Numerical results for phase diffusion time under various conditions indicated. Here ν indicates the mean trap frequency $\omega/2\pi$. Open circles use $\omega_x = \omega_y = \lambda\omega_z$ for $\lambda = 5$, and closed squares use $\lambda = 1$. The solid curves show the approximate Thomas-Fermi result and the dashed curves show the weakly interacting approximation.

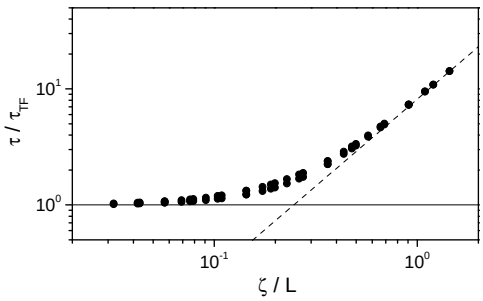

FIG. 5: Relation between phase diffusion time and the Thomas-Fermi parameter ζ/L, where ζ is the healing length and L is the Thomas-Fermi radius. The data are scaled by the Thomas-Fermi diffusion time from (9), and the solid line shows $\tau = \tau_{TF}$. The dashed line shows the weak-interaction approximation of (10). Data points show calculated results for a mix of asymmetries $\lambda = 1$ and $\lambda = 5$.

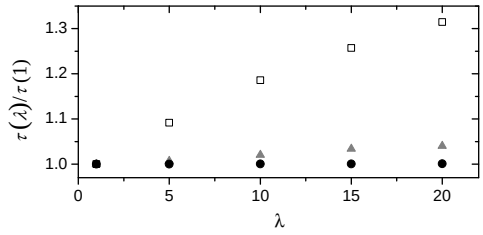

FIG. 6: Dependence of diffusion time $\tau(\lambda)$ on trap symmetry $\lambda = \omega_x/\omega_z$ for a cylindrical trap with $\omega_x = \omega_y$. Values are scaled by the diffusion time for a symmetric trap, $\tau(1)$. Different symbols are calculated for different interaction strengths, as characterized by the ratio of the healing length ξ to the trap size ℓ. Circles have $\xi \approx 5\ell$, squares have $\xi \approx 0.2\ell$, and triangles have $\xi \approx 0.03\ell$.

is large. To illustrate this, Fig. 5 plots the ratio $\tau/\tau_{\rm TF}$ as a function of ζ/L, where $L = (L_x L_y L_z)^{1/3}$ is the mean condensate size. Here we used the Thomas-Fermi approximations for ζ and L, via [16]

$$L = (15Na\ell^4)^{1/5} \tag{12}$$

and the peak density

$$n = \frac{1}{8\pi}\frac{L^2}{a\ell^4}, \tag{13}$$

from which $\zeta/L = (\ell/15Na)^{2/5}$. As seen, the diffusion time can be rather accurately represented as a function of the single variable ζ/L.

In both the strong and weak interaction limit, the diffusion time is independent of the trap symmetry. A weak dependence is observed, however, in the crossover region. This is illustrated in Fig. 6.

V. IMPACT ON EXPERIMENTS

Table I shows the parameters used and coherence times obtained in several experimental implementations, including the most recent results from our own group. As seen from the ζ/L values, all of these experiments are in the crossover regime where the predicted coherence time is somewhat longer than either the Thomas-Fermi or weak interaction formulas would predict.

A long phase diffusion time is of course beneficial, but as can be seen from the table, experiments to date have mostly been instead limited by technical noise sources. The work by Segal *et al.* [22] is a notable exception. The measurement time in that experiment is close to the predicted diffusion time, and in fact exceeds the approximate Thomas-Fermi result of 0.19 s. In that experiment, the interferometer did not exhibit a stable output, but fluctuated from one run to the next. The IZ theory predicts such behavior when the measurement time approaches the diffusion time. However, the observed fluctuations could also be explained by technical sources [22].

Our results do suggest that substantial performance improvements are possible. For instance, if a system similar to our current one were configured to give a loop ge-

Reference	ν_x (Hz)	ν_y (Hz)	ν_z (Hz)	N	T (s)	τ (s)	ζ/L
Wang [3, 20]	100	100	5	3000	0.01	0.23	0.14
Garcia [4]	3.3	6	1.2	10,000	0.04	4.6	0.14
Horikoshi [5]	60	60	0.017	3000	0.06	0.17	0.13
Horikoshi [5]	60	60	0.010	3000	0.1*	0.23	0.14
Burke [21]	3.3	6	1.1	30,000	0.9*	4.8	0.09
Segal [22]	80	80	4.1	3000	0.24*	0.30	0.14
Current	3	5	0.2	10,000	0.10	13.5	0.16

TABLE I: Summary of experimental atom interferometer performance, compared to calculated diffusion times. All results are for ^{87}Rb atoms. Here the ν_i are the trap frequencies, N the atom numbers, and T the experimental measurement time. The asterisks denote measurements exhibiting interference with uncontrolled shot-to-shot phase fluctuations. Our calculated diffusion times are τ, and ζ/L parametrizes the relative strength of interactions.

ometry with a 2-cm radius and a 10-s coherence time, a single shot-noise limited measurement would have a Sagnac rotation sensitivity of about 3×10^{-9} rad/s.

VI. CONCLUSIONS

We have elaborated on Ilo-Okeke and Zozulya's analysis of phase diffusion in an optically-coupled condensate interferometer, by using a realistic simulation of the Gross-Pitaevskii equation to calculate the dynamical evolution of the interferometer wave packet. We find that the diffusion time is well approximated by a Thomas-Fermi result in the strongly-interacting limit, and by a perturbative result in the weakly-interacting limit. We hope that these results will be of use in designing and interpreting future experiments based on condensate interferometry.

We thank Alex Zozulya for helpful comments. This material is based upon work supported by the National Science Foundation under Grant Number 0969916.

[1] P. R. Berman, ed., *Atom Interferometry* (Academic Press, San Diego, 1997).
[2] A. D. Cronin, J. Schmiedmayer, and D. E. Pritchard, Rev. Mod. Phys. **81**, 1051 (2009).
[3] Y. J. Wang, D. Z. Anderson, V. M. Bright, E. A. Cornell, Q. Diot, T. Kishimoto, M. Prentiss, R. A. Saravanan, S. R. Segal, and S. Wu, Phys. Rev. Lett. **94**, 090405 (2005).
[4] O. Garcia, B. Deissler, K. J. Hughes, J. M. Reeves, and C. A. Sackett, Phys. Rev. A **74**, 031601(R) (2006).
[5] M. Horikoshi and K. Nakagawa, Phys. Rev. Lett. **99**, 180401 (2007).
[6] G.-B. Jo, Y. Shin, S. Will, T. A. Pasquini, M. Saba, W. Ketterle, D. E. Pritchard, M. Vengalattore, and M. Prentiss, Phys. Rev. Lett. **98**, 030407 (2007).
[7] A. S. Arnold and E. Riis, J. Mod. Optics **49**, 5861 (1999).
[8] M. Holland, J. Williams, K. Coakley, and J. Cooper, Quantum and Semiclassical Optics **8**, 571 (1996).
[9] M. Lewenstein and L. You, Phys. Rev. Lett. **77**, 3489 (1996).
[10] E. M. Wright, D. F. Walls, and J. C. Garrison, Phys. Rev. Lett. **77**, 2158 (1996).
[11] T. Wong, M. J. Collett, and D. F. Walls, Phys. Rev. A **54**, R3718 (1996).
[12] Y. Castin and J. Dalibard, Phys. Rev. A **55**, 4330 (1997).
[13] J. Javanainen and M. Wilkens, Phys. Rev. Lett. **78**, 4675 (1997).
[14] A. J. Leggett and F. Sols, Phys. Rev. Lett. **81**, 1344 (1998).
[15] E. O. Ilo-Okeke and A. A. Zozulya, Phys. Rev. A **82**, 053603 (2010).
[16] F. Dalfovo, S. Giorgini, L. Pitaevskii, and S. Stringari, Rev. Mod. Phys. **71**, 463 (1999).
[17] M. L. Chiofalo, S. Succi, and M. P. Tosi, Phys. Rev. E **62**, 7438 (2000).
[18] W. Bao, D. Jaksch, and P. Markowich, J. Comp. Phys. **187**, 318 (2003).
[19] J. H. T. Burke, Ph.D. thesis, University of Virginia (2010).
[20] M. Olshanii and V. Dunjko (2005), eprint cond-mat/0505358.
[21] J. H. T. Burke, B. Deissler, K. J. Hughes, and C. A. Sackett, Phys. Rev. A. **78**, 023619 (2008).
[22] S. R. Segal, Q. Diot, E. A. Cornell, A. A. Zozulya, and D. Z. Anderson, Phys. Rev. A **81**, 053601 (2010).